### Title

Surface adsorption of Nordic aquatic fulvic acid on amine-functionalized and non-functionalized mesoporous silica nanoparticles




### Journal

Environmental Science Nano, 5(9)

### ISSN

2051-8153



### Authors

Jayalath, Sanjaya
Larsen, Sarah C
Grassian, Vicki H



### Publication Date

2018

### DOI

10.1039/c8en00618k

Peer reviewed

Environmental Science Nano

PAPER

View Article Online
View Journal | View Issue





Cite this: *Environ. Sci.: Nano*, 2018, 5, 2162

# Surface adsorption of Nordic aquatic fulvic acid on amine-functionalized and non-functionalized mesoporous silica nanoparticles†

Sanjaya Jayalath, [a] Sarah C. Larsen *[a] and Vicki H. Grassian *[b]

Received 9th June 2018,
Accepted 30th July 2018

DOI: 10.1039/c8en00618k

rsc.li/es-nano

Mesoporous silica nanoparticles (MSNs) have the potential to be released into the environment and to then adsorb natural organic matter. Understanding the molecular–surface interactions that drive the kinetics and thermodynamics of the adsorption process is an important goal in developing models that accurately predict the fate and transport of these porous nanomaterials. Motivated by this goal, the adsorption of Nordic aquatic fulvic acid on amine functionalized and non-functionalized MSNs as a function of pH (3, 6 and 8) was studied using attenuated total reflectance Fourier transformation infrared spectroscopy. According to these results, carboxylic acid functional groups of Nordic aquatic fulvic acid and the amine functional groups on the functionalized MSNs play key roles in the adsorption process. Quantitative measurements were conducted using thermogravimetric analysis to determine the surface coverage of fulvic acid on the MSNs. The fulvic acid adsorption was pH dependent and decreased with increasing pH. Amine-functionalized MSNs exhibited a higher adsorption capacity of fulvic acid compared to the non-functionalized nanoparticles under all conditions. Furthermore, zeta potential measurements showed the impact of fulvic acid adsorption on the surface charge for these MSNs. Strikingly, the surface charge changed upon fulvic acid adsorption for amine-functionalized MSNs but remained constant for the unfunctionalized MSNs. Reasons for these differences and the overall environmental implications of this study are discussed.

### Environmental significance

Mesoporous silica nanoparticles (MSNs) have the potential to be released into the environment and adsorb natural organic matter (NOM). The major conclusions of this study are that the extent of adsorption of NOM depends on surface functionalization and solution pH with amine-functionalized MSNs exhibiting: (i) a higher adsorption capacity of NOM compared to the non-functionalized nanoparticles under all conditions; (ii) significantly different changes in zeta potential; (iii) specific electrostatic interactions and; (iv) acid–base chemistry. Overall, understanding the molecular–surface interactions that drive the kinetics and thermodynamics of the adsorption process is an important goal in developing models that accurately predict the fate and transport of these porous nanomaterials in the environment.

## Introduction

Mesoporous silica nanoparticles (MSNs) are versatile materials that are being developed for a variety of applications, such as targeted drug delivery, catalysis, cell labelling and imaging.[1–6] MSNs have desirable properties including high surface areas and tunable pore sizes (2 to 10 nm)[7,8] that make them ideal materials for use in consumer products, thus increasing the potential for MSNs to be released into the environment.

Following release into the environment, MSNs interact with complex environmental and biological milieu which can lead to various nanoparticle transformations, such as adsorption of natural organic matter present in the environment. The nature of the nanoparticle surface in combination with the factors in the surroundings often controls the fate and transport of these materials as well as their interaction with biological organisms. This suggests that surface adsorption processes can alter the fate and transport of MSNs in the environment. In particular, surface adsorption with environmentally relevant ligands, *e.g.* fulvic acids (FA) can occur and alter the surface of the nanoparticles. FA is the most soluble and structurally smallest component of natural organic

[a] *Department of Chemistry, University of Iowa, Iowa City, Iowa 52242, USA. E-mail: sarah-larsen@uiowa.edu*
[b] *Departments of Chemistry & Biochemistry, Nanoengineering and Scripps Institution of Oceanography, University of California San Diego, La Jolla, CA 92093, USA. E-mail: vhgrassian@ucsd.edu*

† Electronic supplementary information (ESI) available. See DOI: 10.1039/c8en00618k

matter (NOM) and is one of the most abundant natural ligands in the environment.[9] FA is difficult to characterize but is known to contain multiple functional groups including carboxylic acids, alcohols and other oxygen containing functional groups as shown Fig. 1.[10] Due to the presence of multiple aromatic and aliphatic carboxylic acid functional groups, FA is known to function as a polyprotic weak acid in the environment.[11–13]

It is well known that FA is capable of coordinating with metal ions to form stable complexes *via* carboxylate functional groups.[10,14] Furthermore FA is also capable of adsorbing onto different mineral surfaces in the environment.[15–18] A Previous study by Liang and coworkers has shown that FA adsorbs on silica nanoparticles. They studied humic acid (HA) and FA adsorption on the surface of different sized silica particles and found that smaller particles showed higher adsorption affinity for FA. Furthermore it was found that FA adsorption on silica is not affected by the ionic strength of the medium.[19] These previous studies suggest that FA adsorption occurs on silica nanoparticle surfaces under a broad range of environmental conditions. However, the impact of pH on the surface adsorption of FA on MSN has not been previously investigated.

In addition, the issue of how surface functionalization of MSNs affects FA adsorption on MSN surface has not been explored. Because functional groups present on the surface of the nanoparticle dictates the surface chemistry of the nanoparticles, understanding surface functionalization and how it changes the interaction of the nanoparticles with the surrounding environmental and biological milieu is an important aspect of eco-toxicity of MSNs. Surface functional groups affect the surface charge of MSNs in aqueous media at varying pH as shown in Fig. 2. Moreover, many applications of MSNs require surface modifications such as amine functionalization to tailor the properties of the MSNs. Prior studies have used amine surface modifications to achieve the slow release of drugs, such as ibuprofen and aspirin from MSNs.[2,20] Therefore, studying the environmental transformations of surface modified MSNs is important in order to better understand the eco-toxicity of MSNs.

In this study, the adsorption of Nordic aquatic fulvic acid (NAFA) on aminopropyltriethoxysilane (APTES)-functionalized and non-functionalized MSNs, denoted as MSNs@APTES and MSNs throughout, under different pH conditions was investigated in order to understand how surface functionalization and pH impact NAFA adsorption. Attenuated total reflectance Fourier transformation Infrared (ATR-FTIR) spectroscopy was used as the primary spectroscopic tool to investigate the mechanism of adsorption on functionalized and non-functionalized MSNs. In these experiments, adsorption of NAFA was studied on a thin film of MSN deposited onto an ATR crystal. This can be viewed as analogous to the surface of a MSN aggregate. Additionally, thermogravimetric analysis (TGA) was used for the quantitative study of NAFA adsorption on functionalized and non-functionalized MSNs. Zeta potential measurements were conducted to assess the impact of NAFA adsorption on surface charge of the functionalized and non-functionalized MSNs. Surface functional groups and adsorbed molecules determine the surface charge of MSNs in aqueous environments. Fig. 2 shows how the silanol groups on non-functionalized MSN and $NH_2$ groups and silanol groups on functionalized MSN affect their surface charge as a function of pH.

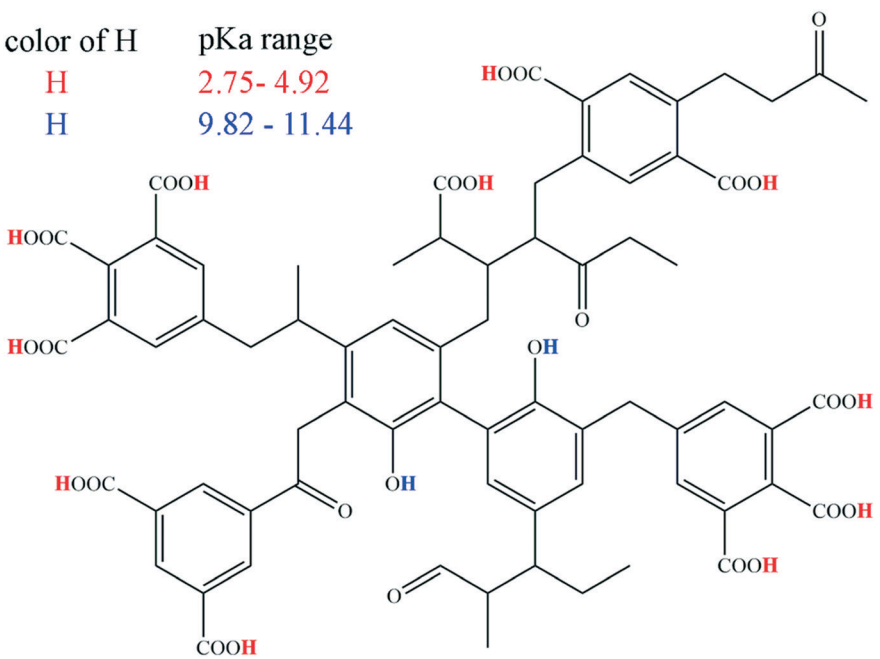


**Fig. 1** Schematic pictorial representation (pseudostructure) of the Nordic aquatic fulvic acid with the range of p$K_a$ values of the most acidic protons.[11]

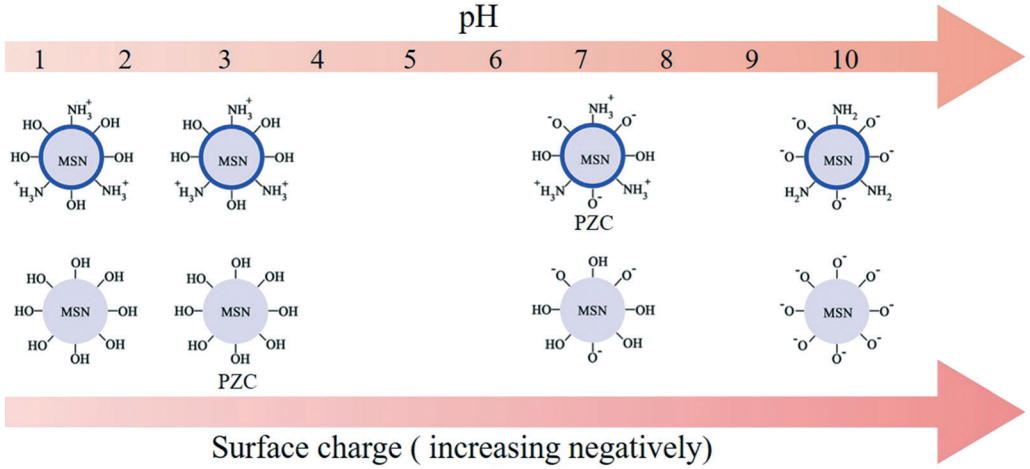


Fig. 2 Depiction of the variation of the surface charge of MSN with pH, based on the surface chemistry of the aminopropyltriethoxysilane (APTES)-functionalized and non-functionalized MSNs, MSNs@APTES and MSNs, respectively.

## Methods and materials

### Attenuated total reflectance-Fourier transformation spectroscopy

ATR-FTIR studies were carried out using Nicolet 670 FTIR spectrometer equipped with a horizontal ATR element. A horizontal flow cell (Pike tech.) with an AMTIR crystal was used for the study. A thin film of silica nanoparticles was drop casted on the crystal using a nanoparticle suspension (2.5 mg $mL^{-1}$). Millipore water was flowed (0.5 mL $min^{-1}$) over the dry film for 60 minutes to remove loosely bound nanoparticles. A flow (0.5 mL $min^{-1}$) of a solution of NAFA (100 mg $L^{-1}$) at the desired pH was passed over the sample for 180 minutes and spectra were collected at 5 minute intervals. The experiments were carried out for both functionalized and non-functionalized silica nanoparticles under three different pH conditions, 3.0, 6.0 and 8.0.

### Thermogravimetric analysis

MSNs (25 mg) were suspended in a 10 mg $mL^{-1}$ NAFA solution (1 mL) for 24 hours in order to achieve maximum adsorption. After 24 hours, the suspension was centrifuged for 5 minutes at 13000 rpm and the supernatant was discarded. NAFA adsorbed nanoparticles were then washed with Millipore water (2 mL) and centrifuged to recover the NAFA adsorbed MSNs. After 3 washing cycles, the MSNs were oven dried (80 °C) for 24 hours. The adsorption experiments were carried out under 3 different pH conditions using both functionalized and non-functionalized MSNs. TGA heating ramp experiments were carried out in a TA 5000 TGA instrument. The NAFA adsorbed samples were heated from 20 °C to 900 °C with a heating rate of 5 °C $min^{-1}$ under $N_2$ purge. NAFA adsorbed functionalized and non-functionalized silica nanoparticles at different pH were analyzed by using the above method. Free MSNs were also analyzed and were subtracted from corresponding NAFA adsorbed MSN to improve the accuracy. All the measurements were triplicated.

### Zeta potential study

The zeta potential measurements were conducted using Malvern Zetasizer Nano-s instrument. pH-adjusted (3.0, 6.0, 8.0) solutions of MSN and MSN@APTES (100 mg $L^{-1}$, 10 mL) were prepared with (100 mg $L^{-1}$) and without (0 mg $L^{-1}$) NAFA in scintillation vials. Ionic strength of the suspensions was kept constant at using $KNO_3$ (10 mM). The pH was adjusted using 1 M NaOH and HCl solutions. These suspensions were then sonicated for 1 h and allowed to stand for 4 h before the zeta potential measurements. The zeta potential measurements were done for each sample and at each pH.

### Materials

NAFA was purchased from International Humic substances society. Mesoporous silica nanoparticles (MSNs) were synthesized, and functionalized with aminopropyltriethoxysilane (APTES) to obtain MSN@APTES. Synthesis, functionalization and characterization were previously reported.[21] MSNs contain only surface silanol groups whereas MSN@APTES have propylamine functional groups decorating the outer surface along with some remaining silanol groups on the surface. The functional group loading of the MSN@APTES was 4.28 mmol $g^{-1}$ and it was determined that these two MSNs, which differ in their surface functionality have approximately the same size distributions and pore diameters. The average size of these MSNs is 50 nm and the average pore diameter is 2 nm. Specific surface area of the MSN was higher (1100 $m^2$ $g^{-1}$) compared to MSN@APTES (700 $m^2$ $g^{-1}$). Additional detailed characterization data of these materials can be found in ref. 21. All solutions were prepared using Millipore water.

 

## Results and discussion

### Overview of APTES-functionalized and non-functionalized MSNs

Functional groups on nanoparticle surfaces control important properties such as surface charge and reactivity. In aqueous solutions, protic functional groups become protonated or deprotonated depending on the pH and p$K_a$ of the acidic group. The FTIR spectra collected of MSN and MSN@APTES (Fig. 3) show IR absorption bands for Si–O–Si asymmetric stretching vibrations (1095 $cm^{-1}$) and Si–O–H bending vibrations (971 $cm^{-1}$). Apart from these IR absorption bands, the spectrum of MSN@APTES shows IR absorption peaks that can be assigned to $NH_2$ (1594, 3361 and 3459 $cm^{-1}$) and $CH_2$ (2879 and 2931 $cm^{-1}$) vibrations of the surface aminopropyl groups.[22] A band for MSN spectrum at 3737 $cm^{-1}$ is assigned to the O–H stretching vibrations of isolated Si–OH groups and the broader band to lower frequency, at 3534 $cm^{-1}$, is due to hydrogen-bonded Si–OH groups.[23–25] For MSN@APTES surface, there are no isolated Si–OH groups present in the spectrum. This indicates that isolated silanol groups either function as grafting sites for aminopropyl groups during functionalization or form hydrogen bonds with surface aminopropyl groups in MSN@APTES.[22] A broader absorption peak appears in the 3700–3500 $cm^{-1}$ region and is assigned to hydrogen bonded silanol groups such as, vicinal and geminal silanol groups present in both types of MSN.[23,25] Absorption bands redshifted from that, near 3361 $cm^{-1}$ are due to N–H stretches in the amine group and bands present in at 2931 and 2879 $cm^{-1}$ are due to C–H stretching vibrations in the aminopropyl groups.[22]

### Solution phase FTIR spectroscopy of NAFA as a function of pH

As shown in Fig. 1, FA contains many functional groups that includes carboxylic and phenolic groups and represents the simplest and the most soluble form of NOM. FA is ubiquitous natural organic matter, but its structure is not specific and, therefore, the exact composition of FA differs from place to place. NAFA, the FA used here, has about 3 times higher carboxylic functional group content than phenolic groups.[11] However, even though the structure and composition of FAs are not exactly the same, carboxylic acids and phenols are the most abundant functional groups in any type of FA. FTIR spectra have been reported for other FA types.[18,26,27] In Fig. 4, the FTIR spectra of NAFA (10 mg $mL^{-1}$) at three pH values are shown. FTIR band frequencies and changes in the frequencies as a function of pH are used to determine corresponding functional groups within NAFA. The infrared absorption band at 1717 $cm^{-1}$ can be assigned to the C=O stretching vibrational mode of carboxylic functional groups and the band decreases in intensity as a function of increasing pH. At pH 3.0, this 1717 $cm^{-1}$ band is the most intense band in the spectrum, but at pH 6.0 and pH 8.0, the intensity of the 1717 $cm^{-1}$ band is gradually reduced in intensity. The observed decreasing trend in absorption band intensity is due to the deprotonation of carboxylic functional groups as the pH increases. A shoulder at higher frequency near 1752 $cm^{-1}$ is assigned to the carbonyl C=O vibrational mode of other carbonyl groups in NAFA such as ester groups which are not affected by pH. The intensity of the 1752 $cm^{-1}$ band is approximately constant with pH. The two absorption bands at 1575 $cm^{-1}$ and 1391 $cm^{-1}$ show an increase in intensity as a function of pH. These two bands are assigned to asymmetric and symmetric stretching vibrational modes of carboxylate ($COO^-$) groups, respectively, due to extensive deprotonation of the carboxylic groups at higher pH. The absorption band at 1594 $cm^{-1}$, which appears in the NAFA spectrum at pH 3.0 is assigned to the asymmetric ring breathing mode of aromatic groups in NAFA.

### Adsorption of NAFA on MSN@APTES and MSN as a function of pH

NAFA adsorption on MSN@APTES and MSN was studied using *in situ* ATR-FTIR that enables monitoring the

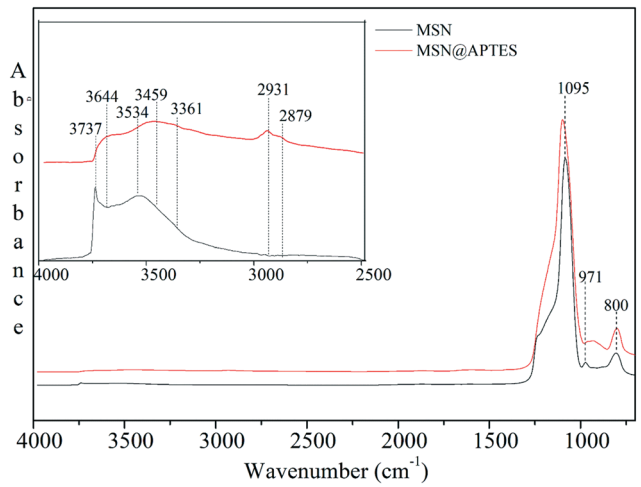


Fig. 3 IR absorption spectra of two types of MSN (shown in red is MSN@APTES and MSN is shown in black). The bands in the range from 2500 to 4000 $cm^{-1}$ can be used to identify different surface functionalities present on these two nanoparticles (see text for additional details).

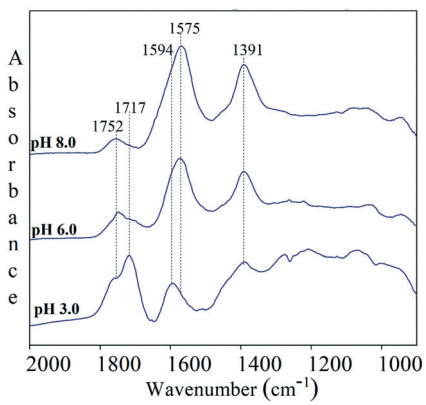


Fig. 4 ATR-FTIR spectra of NAFA solutions (~10 mg $mL^{-1}$) under different pH conditions (3.0, 6.0 and 8.0).

adsorption process in real time. FTIR spectra were collected as NAFA adsorption occurs on MSN thin film surfaces, which is seen in the time dependent IR absorption spectra shown in Fig. 5. Molecular-level information is revealed by comparing the spectra of adsorbed NAFA with the solution phase NAFA spectra discussed in detail above. The spectra collected at early times during the initial stages of adsorption at pH 3.0 on MSN@APTES are very different compared to the corresponding solution phase spectra indicating strong surface complexation of NAFA on the surface of MSN@APTES. The C═O peak that is dominant in solution phase spectra is replaced by two peaks assigned to $COO^-$ symmetric and asymmetric stretch vibrations during the initial stages of NAFA adsorption. This indicates that carboxylic acid groups are deprotonated upon surface adsorption at low pH of 3.0. Adsorption of three small aromatic organic acid model compounds was also studied to facilitate the interpretation of the spectra of adsorbed NAFA. These spectra are shown in ESI† (Fig. SI-1) and provide additional insight into the role of amine groups in the deprotonation of COOH for the small aromatic organic acid model compounds in that all of these are deprotonated on the MSN@APTES surface at pH 3.0. MSN@APTES surface bares a significantly high positive charge at pH 3.0 that can lead to a decrease in proton activity in the electrical double layer near the surface by repelling away the protons. This will generate a relatively higher interfacial pH that depends on the solution pH and the potential drop from the aqueous phase to the interface.[28] Resulting high interfacial pH can promote the deprotonation of the acidic carboxylic functional groups on MSN@APTES surface. This mechanism is previously proposed by Yoon *et al.* to explain the surface induced deprotonation of FA on boehmite surface.[15]

Considering the adsorbed NAFA FTIR spectra of MSN@APTES at longer times, there appear to be protonated COOH groups upon additional adsorption of NAFA. The C═O peak becomes visible in the absorption spectra along with the symmetric and asymmetric peaks associated with

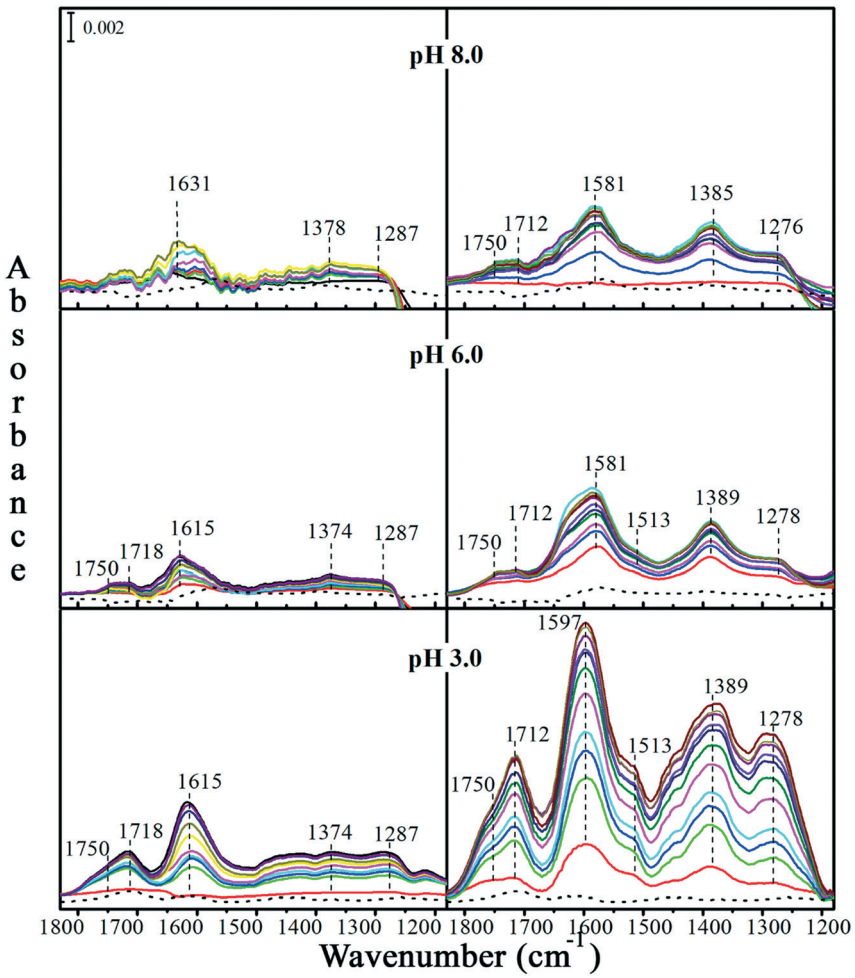


**Fig. 5** ATR-FTIR spectra showing NAFA adsorption on MSN (left panel) and MSN@APTES (right panel) under 3 different pH conditions as a function of time. Dotted line spectra show the solution phase spectra of NAFA at the same pH and concentration (100 mg $L^{-1}$) used for this adsorption study (the dotted line is for solution phase NAFA and shows at this concentration there are minimal contributions of absorption bands from solution phase molecules). Adsorbed phase spectra presented are collected in 5 min intervals during first 30 min and then after in 30 min intervals for 150 min.

 

$COO^-$ groups. This C=O peak can be assigned to carboxylic groups present in adsorbed NAFA molecules that are not bound directly to the surface, possibly due to steric effects. NAFA is a relatively large molecule with a rigid structure that can hinder some carboxylic groups from interacting directly with the surface during adsorption.[19] Interestingly, later stages of adsorption show that there can be multilayer adsorption due to the interactions with strongly adsorbed NAFA and NAFA molecules in a second layer that results in an increase in intensity of C=O vibrations. Multilayer adsorption has also been suggested for NOM adsorption on other inorganic surfaces at low pH.[29–31] Another difference in the spectra of adsorbed NAFA on MSN@APTES compared to solution phase NAFA at pH 3.0 is the presence of an absorption band at 1278 $cm^{-1}$ instead of the broad IR spectral features in the range from 1100 to 1300 $cm^{-1}$ that is seen in the solution phase NAFA spectrum. This broad region contains many vibrational frequencies such as the bending modes of phenol OH, alcohol OH and aliphatic CH groups. Appearance of a distinct peak at 1278 $cm^{-1}$ can be a result of the formation of hydrogen bonds between phenolic groups and the MSN@APTES surface where protons in phenolic groups form hydrogen bonds with acceptor atoms such as O and N present on the MSN@APTES surface.

Band frequencies in adsorbed NAFA spectra on non-functionalized MSNs are comparable to that of the solution phase NAFA spectra as seen in Fig. 5. However, the relative peak intensities are different from that of the solution phase spectra indicating specific interactions with the MSN surface. The most prominent peak in adsorbed NAFA on non-functionalized MSNs is around 1615 $cm^{-1}$ and can be assigned to ring stretching vibrations of aromatic groups whereas in the solution phase C=O peak of COOH groups at 1717 $cm^{-1}$ is the most prominent peak. This difference in intensities between adsorbed and solution phase could be a result of hydrophobic interactions between aromatic functional groups and the MSN surface. At pH 3.0 MSN surface has a net zero charge (pzc of MSN is around pH 3) H-bonding interactions between protonated COOH groups and phenolic groups of NAFA and the MSN surface *via* hydrogen bonds can occur at pH 3.0. These multiple interactions with NAFA molecules suggests strong interactions with the MSN surface, which can impact both vibrational frequencies and intensities from that of the solution phase spectrum at pH 3.0 as observed. However, at higher pH, where COOH groups are deprotonated, the contribution of hydrogen bonds between COOH groups and MSN surface to the adsorption will be diminished lowering the adsorption of NAFA considerably. There will still be some hydrogen bonds formed between phenolic groups and the MSN surface that can be used to account for the adsorption that takes place at higher pH values of 6.0 and 8.0. Apart from this, previous studies have also suggested cation bridges as a possible mechanism for both humic and fulvic acid adsorption on silica surfaces especially at higher pH where both the surface and adsorbates are negatively charged.[19] Most interesting, is that surface induced deprotonation is *not evident* for NAFA adsorbed on the non-functionalized MSN at pH 3.0, which is in stark contrast to what is observed for MSN@APTES. This difference can be explained by the difference in the surface charge of the MSN compared to MSN@APTES. MSN has approximately zero surface charge at pH 3.0 which is not sufficient to generate the higher interfacial pH at the surface that is required to promote the surface induced deprotonation.

The infrared spectra suggest that NAFA adsorption on MSN@APTES is higher than that on MSN at all pH values studied due to the greater intensity of the absorption bands. Overall, the band intensity for NAFA adsorbed on MSN@APTES is higher by at least a factor of two compared to unfunctionalized MSNs at all pH conditions studied. The higher degree of adsorption can be ascribed to the amine functional groups present in MSN@APTES that alter the reactivity and surface charge of MSNs. The amine groups allow the formation of much stronger specific interactions with the functional groups in NAFA such as carboxylic groups compared to relatively weaker interactions between the silanol groups and NAFA. This is also the reason that MSN@APTES materials are used in many more applications compared to non-functionalized MSNs. For example, it has been observed that more ibuprofen can be loaded in amine functionalized MCM-41 nanoparticles compared to bare MCM-41 nanoparticles due to the stronger interaction between COOH and $NH_2$ groups.[2] In related $^{13}C$ NMR experiments, a drastic reduction of the mobility of ibuprofen has been observed in the presence of MSN@APTES suggesting stronger interactions between amine functionalized MSNs and the COOH moieties in ibuprofen.[32] Therefore, this suggests here that there are much stronger interactions between NAFA and MSN@APTES due to the multiple COOH moieties present in the NAFA structure and specific acid–base interactions with amine and COOH groups.

### Quantification of NAFA adsorption on MSN by thermogravimetric analyses

Due to the experimental limitations such as loss of MSN during the experiment and absence of simpler means for the calibration of adsorbed phase, ATR-FTIR analysis was not used for the absolute quantification of the NAFA adsorption on MSN. Instead, quantitative determination was carried out using TGA. NAFA adsorbed on functionalized and non-functionalized MSN at different pH were subjected to TGA analysis and the calculated average NAFA mass loadings are shown in Fig. 6. The highest mass loading of 39.5 mg $g^{-1}$ was observed for MSN@APTES at pH 3.0 and the lowest mass loading of 6 mg $g^{-1}$ was observed for MSN at pH 8.0. These mass loadings are comparatively smaller than the values reported in the literature for a similar study where the reported mass loading was 77 mg $g^{-1}$ for silica nanoparticles with a diameter of 100 nm at pH 4.0 (ref. 19) compared to bare MSN which has an average mass loading

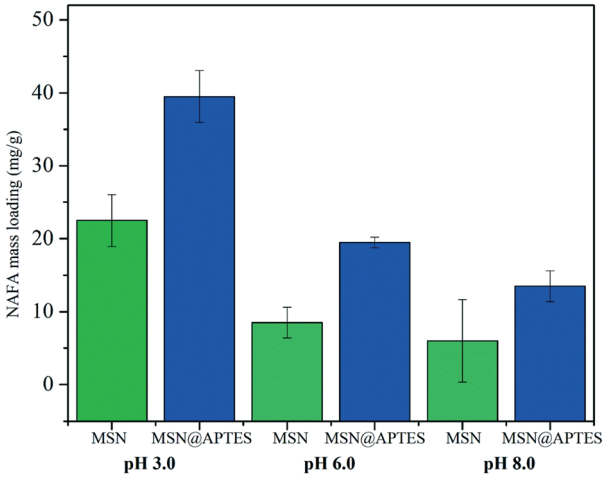


Fig. 6 Average NAFA mass loading (mg $g^{-1}$) of functionalized and non-functionalized MSN at three different pH conditions. Error bars represents standard deviation.

of 22.5 mg $g^{-1}$ at pH 3.0. However, it should be noted that the silica nanoparticles used in this previously reported study were not mesoporous and the type of FA used was also different. The O/C mass ratio of NAFA (this study) is much higher (0.86) compared to that of the FA used in the prior study (0.67) and the method of analysis was also different (total C content *vs.* TGA). MSN@APTES shows relatively higher mass loading than MSN at all the pH conditions studied. The highest difference between mass loadings of NAFA on two types of MSN was observed at pH 3.0. It was 17 mg $g^{-1}$ and was significantly different according to the two-sample *t*-test ($p$ = 0.04). The difference observed at pH 6.0 (11 mg $g^{-1}$) was also significantly different ($p$ = 0.02). However, the difference observed at pH 8.0 was 7.5 mg $g^{-1}$ and it was not significantly different ($p$ = 0.22) according to the two-sample *t*-test. NAFA mass loading shows a decreasing trend as a function of pH that qualitatively agrees with the peak height differences observed in adsorption spectra.

NAFA adsorption varies as a function of pH in both MSN and MSN@APTES. The degree of adsorption decreases at higher pH. This indicates that electrostatic interactions play a role in NAFA adsorption on both MSN@APTES and MSNs. The surface charge of the MSNs and the speciation of NAFA molecules both vary with pH. Electrostatic interactions between charged groups of opposite signs such as between the MSN surface and NAFA, increase the adsorption at low pH. In contrast, at higher pH both the surface and NAFA have more negatively charged sites that therefore causes repulsive interactions and decreases the amount of adsorption at higher pH relative to lower pH values. Similar observations have been reported in other NOM adsorption studies on inorganic surfaces including, iron oxide, silica, titania and alumina.[30,33,34] These observations can be understood further through zeta potential measurements under different pH conditions that provide more detail about surface charge of the MSNs at different pH and the impact of how the surface charge changes with pH.

### Zeta potential measurements

Zeta potential measurements were carried out to analyze the effects of surface adsorbed NAFA on the surface charge of functionalized and non-functionalized MSN. Zeta potential changes can be used to explain the quantitative differences between the NAFA adsorption on MSN and MSN@APTES in terms of the electrostatic interactions. Fig. 7 shows variation of the zeta potential of the MSN (left panel) and MSN@APTES (right panel) before and after NAFA adsorption as a function of pH. The zeta potential of the MSNs was almost zero at pH 3.0 and became more negative as a function of pH due to deprotonation of surface silanol groups at higher pH conditions which increases the negative charge density on the MSN surface. For most MSNs, point of zero charge (pzc) is close to pH 3.[35] In contrast, MSN@APTES has the highest average zeta potential at pH 3.0 (47 mV), which decreases as a function of pH and becomes negative at pH 8.0. The presence of the $NH_2/NH_3^+$ groups alters the surface charge of MSN@APTES due to the positive charges present on protonated $NH_3^+$ groups below the p$K_a$ which is approximately 10.5.[36] The pzc of MSN@APTES is therefore much higher (~pH 6.5) compared to MSNs. Positive charges on the MSN@APTES surface at low pH can interact with deprotonated NAFA molecules *via* electrostatic interactions between surface $NH_3^+$ and $COO^-$ groups of NAFA. At pH 3.0 there are both protonated (COOH) and deprotonated carboxylic ($COO^-$) groups present in NAFA. These $COO^-$ groups will form specific electrostatic interactions with $NH_3^+$ groups on the MSN@APTES surface as denoted in eqn (1). Since the silanol groups of MSN@APTES are protonated, there will be no electrostatic repulsions between NAFA and surface. However, with increasing pH, negative charges on the surface increase due to the deprotonation of surface silanol groups. As a result, electrostatic repulsions between surface silanol groups and $COO^-$ of NAFA on MSN@APTES increase leading to a decreased adsorption with

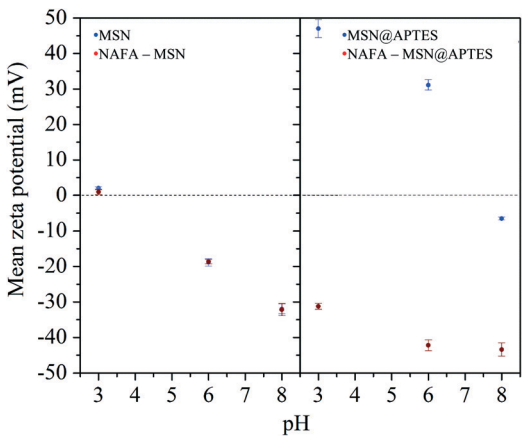


Fig. 7 Mean zeta potential of the NAFA adsorbed and free MSN (left) and MSN@APTES (right) at three different pH. Error bars represents the standard deviation of triplicate measurements.

the increasing pH. In addition, higher zeta potential values means less agglomeration which keeps the available surface area high.

$$m\text{Surface} - NH_3^+ + n\text{NAFA} - COO^- \rightarrow m\text{Surface} - NH_3\cdots OOC + (n-m)\text{NAFA} - COO^- \quad (1)$$

In case of MSN@APTES, adsorption of NAFA dramatically changes the zeta potential at all pH values investigated. At pH 3.0 and 6.0, the zeta potential changes from positive to negative and at pH 8.0, the zeta potential becomes more negative after NAFA adsorption on MSN@APTES. At low pH this surface charge reversal is caused by the surface induced deprotonation that produces multiple $COO^-$ groups in adsorbed NAFA. The degree of the change in zeta potential is highest at pH 3.0 where the degree of adsorption is also the highest. The change in zeta potential decreases as a function of pH in a similar manner to the change in amount of adsorbed NAFA as a function of pH indicating a direct correlation between the zeta potential and adsorbed NAFA. Previous studies have reported similar trends in zeta potential as a function of pH during the adsorption of humic acid on APTES functionalized magnetic silica nanoparticles[37] as well as in charge density as a function of pH during the adsorption of humic acid on silica particles.[38] In contrast to MSN@APTES, there is no difference in zeta potential of NAFA adsorbed MSN at any pH condition studied. This is most likely be due to the relatively lower NAFA adsorption on MSN that is insufficient to create a significant shift in zeta potential. It should be noted that both the adsorption and the shift in zeta potential upon adsorption varies as a function of initial adsorbate to adsorbent ratio in the solution. The concentration of NAFA (100 mg $L^{-1}$) used in zeta potential experiment is smaller than that of the TGA (10 000 mg $mL^{-1}$) studies as well as ATR-FTIR (100 mg $mL^{-1}$ with a continuous flow). Therefore, the amount of NAFA adsorbed could be relatively lower compared to what is observed for the adsorption studies (TGA and ATR-FTIR). Furthermore, at pH 3.0 where the adsorption of NAFA is highest on MSN, the COOH groups remain protonated (no surface induced deprotonation) upon adsorption resulting in no change in the surface charge of the NAFA adsorbed MSN. Similar results were observed during the adsorption of bovine serum albumin (BSA) where there was a larger effect on the zeta potential on MSN@APTES compared to MSN following BSA adsorption.[21] According to classical DLVO theory, increased surface potential leads to stable particles in suspensions. Therefore, NAFA adsorption will further increase the stability of MSN@APTES compared to MSN. Previous studies have shown that the stability of other nanoparticles such as, Au, $TiO_2$ and ZnO in aqueous systems is also increased by NOM adsorbed on the nanoparticle surface.[30,39,40] Moreover the adsorption of MSN@APTES will alter the NOM speciation in the environment especially at lower pH due to the surface induced deprotonation. This can affect the interactions of NOM with other chemical components in the environment such as, heavy metal ions and resulting in complex environmental implications.

# Conclusions and environmental implications

NAFA adsorbs onto both MSN and MSN@APTES surfaces; however, the NAFA adsorption is more prominent on MSN@APTES compared to MSN under all pH conditions (3.0, 6.0, 8.0) studied as monitored by FTIR, TGA and zeta potential. Adsorption of NAFA occurs on MSN@APTES *via* electrostatic interaction and surface complexation between COOH groups of NAFA and $NH_3^+$ groups of MSN@APTES whereas, on MSN, adsorption occurs *via* hydrogen bonding and hydrophobic interactions. The adsorption of NAFA decreases with increasing pH on both unfunctionalized and APTES functionalized MSNs as observed by FTIR and through quantification of the adsorption by TGA. Surface induced deprotonation of NAFA is observed on MSN@APTES at pH 3.0 leading to the highest NAFA adsorption capacity (39.5 mg $g^{-1}$ by TGA) observed in our study. Adsorbed NAFA on MSN@APTES decreases the zeta potential at all pH values studied; however, the zeta potential of MSN is completely unaffected by adsorbed NAFA, most probably due to the lower degree of adsorption and the lack of any electrostatic or acid–base interactions. MSN@APTES nanoparticles with adsorbed NAFA are stable as demonstrated by the highly negative zeta potential under all pH conditions. Importantly, this study demonstrates how surface functionality dictates the extent of adsorption and the interaction with natural organic matter upon adsorption. These results further confirm the need for understanding the detailed molecular–surface interactions in order to develop models that accurately predict the fate and transport of nanomaterials in the environment.

# Conflicts of interest

There are no conflicts to declare.

# Acknowledgements

This material is based on the work supported by the National Science Foundation under grant number NSF CHE-1606607 (VHG) and CHE-1538847 (SCL). Any opinions, findings, and conclusions or recommendations expressed in this material are those of the authors and do not necessarily reflect the views of the National Science Foundation.

# References

1 J. Lu, M. Liong, J. I. Zink and F. Tamanoi, Mesoporous silica nanoparticles as a delivery system for hydrophobic anticancer drugs, *Small*, 2007, **3**, 1341–1346.
2 B. Muñoz, A. Rámila, J. Pérez-Pariente, I. Díaz and M. Vallet-Regí, MCM-41 organic modification as drug delivery rate regulator, *Chem. Mater.*, 2003, **15**, 500–503.
3 S.-H. Cheng, C.-H. Lee, M.-C. Chen, J. S. Souris, F.-G. Tseng, C.-S. Yang, C.-Y. Mou, C.-T. Chen and L.-W. Lo, Trifunctionalization of mesoporous silica nanoparticles for comprehensive cancer theranostics—the trio of imaging, targeting and therapy, *J. Mater. Chem.*, 2010, **20**, 6149–6157.

4 C. H. Lee, S. H. Cheng, Y. J. Wang, Y. C. Chen, N. T. Chen, J. Souris, C. T. Chen, C. Y. Mou, C. S. Yang and L. W. Lo, Near-infrared mesoporous silica nanoparticles for optical imaging: Characterization and in vivo biodistribution, *Adv. Funct. Mater.*, 2009, **19**, 215–222.

5 S. H. Wu, Y. S. Lin, Y. Hung, Y. H. Chou, Y. H. Hsu, C. Chang and C. Y. Mou, Multifunctional mesoporous silica nanoparticles for intracellular labeling and animal magnetic resonance imaging studies, *ChemBioChem*, 2008, **9**, 53–57.

6 D.-M. Huang, Y. Hung, B.-S. Ko, S.-C. Hsu, W.-H. Chen, C.-L. Chien, C.-P. Tsai, C.-T. Kuo, J.-C. Kang and C.-S. Yang, Highly efficient cellular labeling of mesoporous nanoparticles in human mesenchymal stem cells: implication for stem cell tracking, *FASEB J.*, 2005, **19**, 2014–2016.

7 B. G. Trewyn, S. Giri, I. I. Slowing and V. S.-Y. Lin, Mesoporous silica nanoparticle based controlled release, drug delivery, and biosensor systems, *Chem. Commun.*, 2007, 3236–3245.

8 I. I. Slowing, J. L. Vivero-Escoto, C.-W. Wu and V. S.-Y. Lin, Mesoporous silica nanoparticles as controlled release drug delivery and gene transfection carriers, *Adv. Drug Delivery Rev.*, 2008, **60**, 1278–1288.

9 T. A. Jackson, Humic matter in natural waters and sediments, *Soil Sci.*, 1975, **119**, 56–64.

10 J. Reuter and E. Perdue, Importance of heavy metal-organic matter interactions in natural waters, *Geochim. Cosmochim. Acta*, 1977, **41**, 325–334.

11 J. D. Ritchie and E. M. Perdue, Proton-binding study of standard and reference fulvic acids, humic acids, and natural organic matter, *Geochim. Cosmochim. Acta*, 2003, **67**, 85–96.

12 J. Ephraim, S. Alegret, A. Mathuthu, M. Bicking, R. L. Malcolm and J. A. Marinsky, A unified physicochemical description of the protonation and metal ion complexation equilibria of natural organic acids (humic and fulvic acids). 2. Influence of polyelectrolyte properties and functional group heterogeneity on the protonation equilibria of fulvic acid, *Environ. Sci. Technol.*, 1986, **20**, 354–366.

13 D. S. Gamble, Titration curves of fulvic acid: the analytical chemistry of a weak acid polyelectrolyte, *Can. J. Chem.*, 1970, **48**, 2662–2669.

14 F. Stevenson and A. Fitch, Chemistry of complexation of metal ions with soil solution organics, *Interactions of soil minerals with natural organics and microbes*, 1986, pp. 29–58.

15 T. H. Yoon, S. B. Johnson and G. E. Brown, Adsorption of Suwannee river fulvic acid on aluminum oxyhydroxide surfaces: An in situ ATR-FTIR study, *Langmuir*, 2004, **20**, 5655–5658.

16 J. D. Filius, D. G. Lumsdon, J. C. Meeussen, T. Hiemstra and W. H. Van Riemsdijk, Adsorption of fulvic acid on goethite, *Geochim. Cosmochim. Acta*, 2000, **64**, 51–60.

17 R. Amal, J. A. Raper and T. Waite, Effect of fulvic acid adsorption on the aggregation kinetics and structure of hematite particles, *J. Colloid Interface Sci.*, 1992, **151**, 244–257.

18 H. Fu and X. Quan, Complexes of fulvic acid on the surface of hematite, goethite, and akaganeite: FTIR observation, *Chemosphere*, 2006, **63**, 403–410.

19 L. Liang, L. Luo and S. Zhang, Adsorption and desorption of humic and fulvic acids on $SiO_2$ particles at nano-and micro-scales, *Colloids Surf., A*, 2011, **384**, 126–130.

20 L. Gao, J. Sun and Y. Li, Functionalized bimodal mesoporous silicas as carriers for controlled aspirin delivery, *J. Solid State Chem.*, 2011, **184**, 1909–1914.

21 S. E. Lehman, I. A. Mudunkotuwa, V. H. Grassian and S. C. Larsen, Nano–bio interactions of porous and nonporous silica nanoparticles of varied surface chemistry: A structural, kinetic, and thermodynamic study of protein adsorption from rpmi culture medium, *Langmuir*, 2016, **32**, 731–742.

22 Z. Bacsik, N. Ahlsten, A. Ziadi, G. Zhao, A. E. Garcia-Bennett, B. Martín-Matute and N. Hedin, Mechanisms and kinetics for sorption of $CO_2$ on bicontinuous mesoporous silica modified with n-propylamine, *Langmuir*, 2011, **27**, 11118–11128.

23 X. Zhao, G. Lu, A. Whittaker, G. Millar and H. Zhu, Comprehensive study of surface chemistry of MCM-41 using 29Si CP/MAS NMR, FTIR, pyridine-TPD, and TGA, *J. Phys. Chem. B*, 1997, **101**, 6525–6531.

24 D. L. Angst and G. W. Simmons, Moisture absorption characteristics of organosiloxane self-assembled monolayers, *Langmuir*, 1991, **7**, 2236–2242.

25 A. Jentys, N. H. Pham and H. Vinek, Nature of hydroxy groups in MCM-41, *J. Chem. Soc., Faraday Trans.*, 1996, **92**, 3287–3291.

26 T. H. Yoon, S. B. Johnson and G. E. Brown, Adsorption of Suwannee River fulvic acid on aluminum oxyhydroxide surfaces: an in situ ATR-FTIR study, *Langmuir*, 2004, **20**, 5655–5658.

27 G. Ait Baddi, M. Hafidi, J. Cegarra, J. A. Alburquerque, J. Gonzálvez, V. Gilard and J.-C. Revel, Characterization of fulvic acids by elemental and spectroscopic (FTIR and 13C-NMR) analyses during composting of olive mill wastes plus straw, *Bioresour. Technol.*, 2004, **93**, 285–290.

28 R. R. Naujok, D. A. Higgins, D. G. Hanken and R. M. Com, Optical second-harmonic generation measurements of molecular adsorption and orientation at the liquid/liquid electrochemical interface, *J. Chem. Soc., Faraday Trans.*, 1995, **91**, 1411–1420.

29 R. F. Domingos, N. Tufenkji and K. J. Wilkinson, Aggregation of titanium dioxide nanoparticles: role of a fulvic acid, *Environ. Sci. Technol.*, 2009, **43**, 1282–1286.

30 S. Jayalath, H. Wu, S. C. Larsen and V. H. Grassian, Surface adsorption of suwannee river humic acid on $TiO_2$ nanoparticles: A study of ph and particle size, *Langmuir*, 2018, **34**, 3136–3145.

31 J. M. Gorham, J. D. Wnuk, M. Shin and H. Fairbrother, Adsorption of natural organic matter onto carbonaceous surfaces: Atomic force microscopy study, *Environ. Sci. Technol.*, 2007, **41**, 1238–1244.

32 M. Vallet-Regí, Ordered mesoporous materials in the context of drug delivery systems and bone tissue engineering, *Chem. – Eur. J.*, 2006, **12**, 5934–5943.

 

33 K. Yang, D. Lin and B. Xing, Interactions of humic acid with nanosized inorganic oxides, *Langmuir*, 2009, **25**, 3571–3576.
34 B. Gu, J. Schmitt, Z. Chen, L. Liang and J. F. McCarthy, Adsorption and desorption of natural organic matter on iron oxide: mechanisms and models, *Environ. Sci. Technol.*, 1994, **28**, 38–46.
35 L. Chia-Hung, L. Leu-Wei, M. Chung-Yuan and Y. Chung-Shi, Synthesis and characterization of positive-charge functionalized mesoporous silica nanoparticles for oral drug delivery of an anti-inflammatory drug, *Adv. Funct. Mater.*, 2008, **18**, 3283–3292.
36 Y. Tataurova, M. J. Sealy, R. G. Larsen and S. C. Larsen, Surface-selective solution NMR studies of functionalized zeolite nanoparticles, *J. Phys. Chem. Lett.*, 2012, **3**, 425–429.
37 J. Wang, H. Tian and Y. Ji, Adsorption behavior and mechanism of humic acid on aminated magnetic nanoadsorbent, *Sep. Sci. Technol.*, 2015, **50**, 1285–1293.
38 L. K. Koopal, Y. Yang, A. J. Minnaard, P. L. M. Theunissen and W. H. Van Riemsdijk, Chemical immobilisation of humic acid on silica, *Colloids Surf., A*, 1998, **141**, 385–395.
39 A. A. Keller, H. Wang, D. Zhou, H. S. Lenihan, G. Cherr, B. J. Cardinale, R. Miller and Z. Ji, Stability and aggregation of metal oxide nanoparticles in natural aqueous matrices, *Environ. Sci. Technol.*, 2010, **44**, 1962–1967.
40 J. Liu, S. Legros, G. Ma, J. G. C. Veinot, F. von der Kammer and T. Hofmann, Influence of surface functionalization and particle size on the aggregation kinetics of engineered nanoparticles, *Chemosphere*, 2012, **87**, 918–924.